On Flow of Asphalt

F. MOAVENZADEH and R. R. STANDER, JR.
Respectively, Assistant Professor and Research Assistant, Department of Civil Engineering, Massachusetts Institute of Technology, Cambridge

This paper reviews some concepts suggested to analyze the flow characteristics of rheological materials with emphasis on those which are promising in the analysis of flow of asphalts. The suggested concepts are categorized as experimental, mathematical, structural, and physical-chemical. It is shown that for the two asphalts used in this study, it is possible to construct flow diagrams over a wide range of shear stress, rate of shear, and temperature by using three different viscometers and the principle of reduced variables. The application of Eyring's rate process theory to the analysis of asphalt flow is examined and the variation of viscosity, determined at constant shear stress or constant shear rate, with temperature is discussed.

•KNOWLEDGE OF the flow properties of asphaltic materials is of special interest in the design of asphaltic mixtures. Such knowledge should lead to a better understanding of the properties of the asphalt-aggregate mixture which in turn should result in the development of a more rational method of mixture design. An understanding of the effect of loading and climatic variables on the flow properties of the binder could be of great assistance in the selection of the most suitable asphalt for a specified job.

The complex chemical structure and numerous varieties of asphalts have, thus far, prevented development of a specific mechanism for describing its flow behavior over the useful range of loading and climatic variables. There are, however, a great number of empirical models, relatively few semi-empirical models, and few theoretical models proposed to describe the flow behavior of asphaltic materials over a limited range of some specific variables. The extent of work in this area was well reviewed by Schweyer in 1958 (1), who said, "Acceptance of the statement that 'knowledge in a field is measured by the brevity with which the concepts can be presented' makes the asphalt technologist pause when the voluminous literature on asphalt is considered." This, in other words, indicates that the "art of asphalt" is a very real and necessary part of asphalt technology, and in order to achieve a scientific base for this art, fundamental concepts involving the flow properties of asphalt must be developed. Thus, it is the general objective of this paper to contribute to the development of such concepts by briefly reviewing the fundamentals involved in analyzing the flow behavior of materials and discussing the difficulties encountered in their application to asphalt. The response of certain asphalts under loading as measured by different methods is presented and the applicability of some rheologic concepts to the analysis of the results is discussed.

CURRENT TRENDS

The objective of rheology is to yield a distinct fundamental, or rational, description of the deformation and flow of matter. To achieve this end the physical chemist has approached the problem by considering the molecular characteristic of materials. The quantum mechanics mathematician approaches the problem by formulating constitutive

Paper sponsored by Committee on Characteristics of Bituminous Materials and presented at the 45th Annual Meeting.

equations and/or conservation relations for particular materials. Although advances in both of these fields are quite evident, the practical requirements of industry have outrun basic research. This situation has created analytical and empirical solutions based on simplifying assumptions as applied to observed flow conditions. More and more, the applied approach has become that of using as much as possible of the physical-chemical and continuum mechanic works. This is quite evident from the recent works of Herrin and Jones (2) and Majidzadeh and Schweyer(3). The former have used the advances in the application of rate process theory (4) to the rheological studies of asphalt, and the latter have used a kinetic approach (5) to analyze the flow behavior of the asphalt.

FLOW REPRESENTATION

In general, there are two basic methods to represent the flow of a fluid, by using a shear stress-rate of shear diagram or by using a viscosity-shear rate diagram. It might also be argued that the single point viscosity (coefficient of viscosity) is sufficient to represent the data; however, for research purposes, the use of this parameter is limited to Newtonian materials which, unfortunately, do not include a great number of paving asphalts.

The simplest plot of flow data is that of shear stress vs rate of shear on arithmetic coordinates. A Newtonian material will plot as a straight line passing through the origin. If the material is non-Newtonian, the data will, in general, pass through the origin but will not be linear. The disadvantage of this plot is that the degree of deviation from Newtonian characteristics cannot be determined. This can be accomplished in most cases by using a log-log plot. Generally, the data will describe a straight line which may be represented by a power formula

$$\tau = A\ (\dot{\gamma})^n \qquad (1)$$

where n is a measure of the deviation from Newtonian behavior. For a Newtonian material, n is equal to unity.

Consistency cannot be represented by A because of the dimensional difficulties; however, the viscosity, defined as $\tau/\dot{\gamma}$ for a given $\dot{\gamma}$ (sometimes referred to as apparent viscosity), may be used. Since the $\dot{\gamma}$ used is arbitrary, and not standardized, confusion may result. An alternate method is proposed by Traxler (6) in which viscosities are compared at a particular power input per volume of sample. Although the power input is arbitrary ($\tau \times \dot{\gamma}$/unit volume = 1,000 given as convenient), the method has the advantage that very little extrapolation of data is necessary to determine values over a wide range of materials and test temperatures. The degree of data treatment required to arrive at the basic shear stress-rate of shear diagram, generally depends on the geometry of the test apparatus used.

An alternate method of flow representation is in terms of the viscosity-shear rate diagram. For Newtonian materials, viscosity is defined as the ratio of shear stress to shear rate which at constant temperature is independent of the shear stress level. For non-Newtonian materials, the ratio is defined as apparent viscosity, and is shear-dependent. The slope of the shear diagram, also used to define viscosity, is called the differential viscosity, $\eta_D = \partial\tau/\partial\dot{\gamma}$. For a power law material the plots of both apparent viscosity and differential viscosity vs shear rate should be straight and parallel lines. A third term, referred to as plastic viscosity, is defined as the slope of the straight line portion of $\dot{\gamma}$ vs τ on arithmetic scales. This viscosity is independent of shear rate and is generally used to determine the yield stress of pseudoplastic materials.

Materials exhibiting rheologic behavior are usually divided into different groups according to their flow characteristics. The general division is that of Newtonian and non-Newtonian flow behavior. Although Reiner (7) objects to this division and believes that all materials showing viscosity should be called Newtonian fluids, and those with variable viscosity, generalized Newtonian fluids, in most rheologic work and for the purpose of this discussion, the Newtonian and non-Newtonian division is used.

Non-Newtonian flow is generally either shear thinning or shear thickening. The first group would include the ideal Bingham plastic and the pseudoplastics, as they both exhibit

decreasing apparent viscosity with increasing shear rate The term thixotropy, as sometimes applied to this whole group, is used here to describe a special case of shear thinning in that it is time-dependent. The structure, which is broken down by shear, is recoverable with time, or, in other words, the process is reversible. Dilatancy is sometimes used to describe shear thickening material; however, this is a misnomer in that many materials which show increasing viscosity with increasing shear do not dilate at all. Thus, dilatancy is a special case of shear thickening. Another unfortunate misuse of terms results by describing time-dependent, shear thickening behavior as rheopectic. There may exist a material which displays shear thickening with time, but rheopexy is the process by which certain thixotropic materials regain their structure faster with the application of a gentle shear. This is analogous to the flocculation process which is speeded by a gentle stirring action. In both cases, increasing the shear beyond a certain limit will start to destroy the structure.

DATA INTERPRETATION

The basic objective of data interpretation is the prediction of flow properties, given limited information.

Experimental Representation

Until the development of a fundamental concept describing the flow behavior of materials in general, use of the existing models is generally limited to the range of variables incorporated in the development of such models. Thus application of these models, while showing good results when properly employed, is limited to the exact test conditions and materials as those used in the development of the particular relationship. In other words, these equations are usually developed to cover a very specific range of data. This can, perhaps, best be illustrated by allusion to the developments for a pseudoplastic material as defined by the flow diagram below.

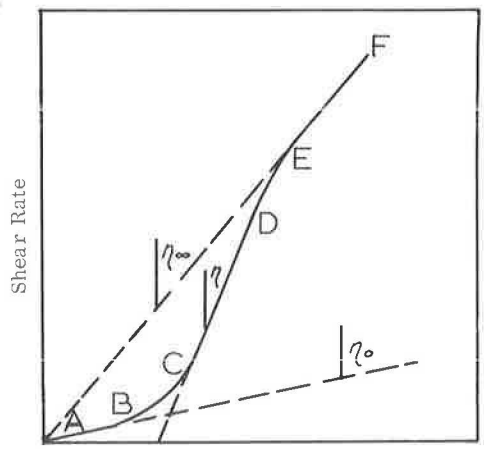

In this figure, the total flow diagram is the line ABCDEF; however, for many cases, description of only part of this line is necessary. For the straight line portion AB, the material is Newtonian and can be described by

$$\tau = \eta_0 \dot{\gamma} \qquad (2)$$

This is again true for EF with η_0 replaced by η_∞ where $\eta_\infty < \eta_0$. In the portion CD, the data are described by the Bingham plastic relationship

$$\tau - \tau_0 = \eta \dot{\gamma} \tag{3}$$

The power function, first proposed by Ostwald and described by Reiner (7) is a good approximation of the portion AC, where

$$\tau = A (\dot{\gamma})^n \tag{4}$$

and n for a pseudoplastic is less than unity. To extend the description to point D, the relationship

$$\dot{\gamma} = A \sinh B \tau \tag{5}$$

gives a very good approximation. Finally, to describe the entire curve, the equation

$$\eta = \frac{(\eta_0 - \eta_\infty)}{1 + A\dot{\gamma} + B\dot{\gamma}^n} + \eta_\infty \tag{6}$$

has been suggested (8).

Each equation is valid only within the range of the variables considered in its development and subsequent substantiation. Each has served and will continue to serve its purpose, but their limitations and conditions must be thoroughly known before they can be applied with meaning.

Mathematical Representation

To examine the flow behavior from the standpoint of continuum mechanics, certain relationships regarding the state of the material must be derived. These equations, commonly called the equations of change, are the relationships for conservation of mass, momentum, and mechanical and thermal energy, each of which is covered for both isothermal and non-isothermal systems.

The general procedure for developing any one of the equations of change is to assume a volume element of dimensions Δx, Δy, and Δz. The flow of the quantity of interest is then formulated for each face of the element, and the dimensions Δx, Δy, Δz are allowed to approach zero. This result, with some simple manipulation, is the final form of interest.

With this general procedure, each case can be taken in turn. For conservation of mass, the mass balance equations result in

$$\frac{\partial \rho}{\partial t} = -(\nabla \cdot \rho v) \tag{7}$$

where $\nabla = \left(\frac{\partial}{\partial x} + \frac{\partial}{\partial y} + \frac{\partial}{\partial z}\right)$. An important form of this equation is for a fluid of constant density, or

$$(\nabla \cdot v) = 0 \tag{8}$$

Considering conservation of momentum, the problem of momentum balance across any face becomes more involved, since momentum terms must be accounted for in all three coordinate directions for each face. The momentum balance equation not only

includes momentum in and out, but also the sum of the forces acting on the face such that

$$\frac{\partial}{\partial t} \rho v = -[\nabla \cdot \rho vv] - [\nabla \cdot \tau] - \nabla p + \rho g \tag{9}$$

where $[\nabla \cdot \rho vv]$ and $[\nabla \cdot \tau]$ are vectors because of the tensoral nature of ρvv and τ. To use Eq. 9 for flow analysis, the expressions for the components of τ must be known. For a Newtonian fluid, they are of the form

$$\tau_{xx} = -2\mu \frac{\partial v_x}{\partial x} + \left(\frac{2}{3}\mu - K\right)(\nabla \cdot v) \tag{10}$$

and

$$\tau_{xy} = \tau_{yx} = -\mu \left(\frac{\partial v_x}{\partial y} + \frac{\partial v_y}{\partial x}\right) \tag{11}$$

where μ and K are the coefficient of Newtonian viscosity and the coefficient of bulk viscosity, respectively. Some authors (9) suggest that the K term can be dropped as negligible, while others (7) are of the opinion that K is of the same order of magnitude as μ.

A useful form of Eq. 9 is for flow between parallel plates

$$\tau_{xx} = \tau_{yy} = \tau_{zz} = \tau_{yz} = \tau_{xz} = 0 \tag{12}$$

and

$$\tau_{xy} = -\mu \left(\frac{dv_x}{dy}\right) \tag{13}$$

which is Newton's law of viscosity.

The rate of change of kinetic energy per unit mass is found by considering the scalar product of local velocity with the equation for conservation of momentum

$$\frac{\partial}{\partial t}\left(\frac{1}{2}\rho v^2\right) = -\left(\nabla \cdot \frac{1}{2}\rho v^2 v\right) - (\nabla \cdot pv) - p(-\nabla \cdot v) - \nabla \cdot (\tau \cdot v) - (-\tau : \nabla v) + \rho(v \cdot g) \tag{14}$$

So far, this analysis is based on an isothermal system; however, the term $(-\tau : \nabla v)$ describes the irreversible conversion of internal energy. Since some mechanical energy is thus obviously degraded to thermal, the system is not strictly isothermal unless an isothermal system is defined as one in which generated heat does not cause appreciable temperature change. This is true in all but high-speed flow systems with large velocity gradients. After examining the equation for mechanical energy, the subject can now be expanded to thermal energy which also allows the examination of non-isothermal systems. Again assuming the general procedure as first set forth, the energy balance equation, including the effects of kinetic and heat energy and the rate of work done on the system, may be written as

$$\frac{\partial}{\partial t} \rho \left(U + \frac{1}{2} v^2\right) = -\left(\nabla \cdot \rho v \left(U + \frac{1}{2} v^2\right)\right) - (\nabla \cdot q) + \rho (v \cdot g) - (\nabla \cdot pv) - (\nabla \cdot [\tau \cdot v]) \tag{15}$$

where U is the internal energy per unit mass of the fluid within the original volume element.

By using the five equations shown here, alone or in combination, flow problems may be set up. With the help of numerous assumptions, the resulting equations may be reduced to a solution. The difficulty in applying the equations of change to practical flow problems is that in all but a few select and simple cases, the simplifying assumptions that are necessary damage the validity of the analysis so much that the results are of questionable value. It is the current trend of research in this area to apply as much as possible the mathematical approach to empirically developed models.

Structural Representation

In recent years, the most promising approach for developing a general theory of flow has been through a structural explanation. Three basic procedures have been suggested depending on whether colloidal theory, rate theory, or kinetic theory is taken as the basis of the argument. The colloidal theory is the oldest and simplest of the three. The approach is based on low concentrations of particles in a solvent. Einstein first deduced the equation

$$\eta = \eta_0 (1 + 2.5 \phi) \tag{16}$$

for solutions below about two-tenths percent of spherical particles. Here, η_0 is the viscosity of the pure solvent and ϕ is the volume of spherical particles per unit volume of suspension. The only assumption is that there is no interaction between the individual spheres. Guth, Gold, and Simha (10) later amended the relationship as

$$\eta = \eta_0 (1 + 2.5 \phi + 14.1 \phi^2) \tag{17}$$

which has been experimentally validated for up to 6 percent solutions. Using the basic idea that relative viscosity—the solution viscosity divided by the solvent viscosity—is a function of the energy dissipation caused by the presence of the suspended particles, relationships have been developed for particles of varied shapes at a range of concentrations. The effects of particle interaction, absorption of the solvent, particle deformability, system thermodynamic conditions, and system electrical conditions are also investigated in the light of colloidal theory (10).

The second approach is that of Eyring and his co-workers. As stated by Brodkey, "their work is based on the application of the theory of rate processes to the relaxation processes that are believed to play an important part in determining the nature of the flow... Very briefly, the theory postulates an activated complex as an intermediate unstable state, which would be formed from the reactants and decompose into the products. The assumption is made that the decomposition of the complex is the rate controlling step, and that there is an activation energy associated with this (11)." To expand this argument, the following is presented as digested from Glasstone et al. (4).

Liquids and gases may be considered as opposites, one consisting of matter moving around holes (gases), and the other, holes moving around matter. The energy necessary to provide molecular movement is made up of two parts, the energy to create a hole, and the energy to move a molecule into it. Taking E as the energy required to vaporize the molecule and leave behind a hole, then $\frac{1}{2}$ E is required if the hole is closed, and E - $\frac{1}{2}$ E or $\frac{1}{2}$ E is required merely to make the hole; $\frac{1}{2}$ E is then the energy of vaporization of the molecule.

In order to extend this development to viscosity, reference is made to the figure on the following page. For a molecule to move the distance δ, it must be transported across an energy barrier, E_0, the energy of activation. The net rate of flow in terms of shear rate is

$$\dot{\gamma} = \frac{2\delta}{\delta_1} k \sinh \frac{F\delta\delta_2\delta_3}{2KT} \tag{18}$$

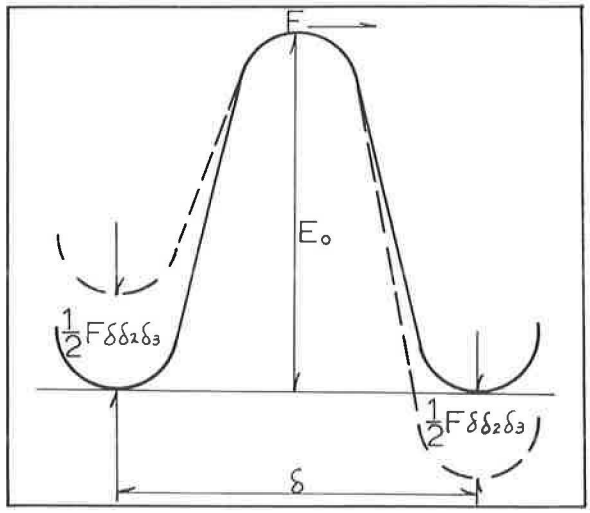

where k is the initial rate of motion and F is the applied shearing force. Using statistical mechanics, k may be shown to be

$$k = \frac{KT}{h} \exp\left(\frac{-E_O}{RT}\right) \tag{19}$$

where K, h, and R are respectively the Boltzmann, Planck, and universal gas constants. Then

$$\dot{\gamma} = A \sinh B\tau \tag{20}$$

where

$$A = \frac{2KT}{h} \exp\left(\frac{-E_O}{RT}\right) \tag{21}$$

and

$$B = \frac{\delta\delta_2\delta_3}{2KT} \tag{22}$$

The third concept of structural flow is that based on a homogeneous reaction kinetic approach as developed by Denny and Brodkey (5, 11, 12). The basic hypothesis is that non-Newtonian behavior is caused by a structural breakdown of the forces between particles. At very low shear rates, the viscosity is a constant, η_O, and at high shear rates, the viscosity of the material again approaches a constant η_∞. These two represent the limiting cases of no breakdown and complete breakdown. At any point between these extremes, the viscosity η is some function of the portion of unbroken forces within the material. By applying the inverse lever principle, the portion of broken forces may be taken as

$$F = \frac{f(\eta_O) - f(\eta)}{f(\eta) - f(\eta_\infty)} \tag{23}$$

and the unbroken portion is 1 - F. The function f (η) is a relationship for the concentration of changing structure to viscosity and for polymer melts and polymers in solution the proper form would be (11)

$$f(\eta) = A\,\eta^{1/3.5} \tag{24}$$

It is noted that all viscosities are the true apparent viscosities, or the arctangent of a straight line drawn from the origin to the point on the flow diagram in consideration.

In order to establish the kinetic reaction rate, consider the reaction

$$\text{unbroken forces} \underset{k_1}{\overset{k_2}{\rightleftharpoons}} \text{broken forces} \tag{25}$$

which has the kinetric reaction equation

$$-\frac{d(1 - F)}{dt} = k_1'(1 - F)^n - k_2 F^m \tag{26}$$

where k_1' must include the effect of shear stress. Therefore

$$k_1' = k_1(\tau)^p \tag{27}$$

Brodkey (11) has suggested the use of shear stress rather than shear rate so as to separate the effect of temperature on viscosity from the effect of shear rate on the structural reaction. The reasoning is that if shear rate is used, then the reaction rate would be affected by both changes in the F and k terms, whereas, if shear stress is used, the F term is constant with constant temperature, and the rate is changed only by changes in the k's.

Following this development, then

$$-\frac{d(1 - F)}{dt} = k_1(1 - F)^n(\tau)^p - k_2 F^m \tag{28}$$

At the limiting viscosity

$$\frac{-d(1 - F)}{dt} = 0 \tag{29}$$

and

$$K = \frac{k_1}{k_2} = \frac{F^m}{(1 - F)^n \tau^p} \tag{30}$$

where K is of the form of an equilibrium constant. The integer constants, m and n, may be taken from initial rates, or in the case of time-dependent materials, by integration with assumed values for m and n along a constant shear line.

The attractions of this theory are that the exact nature of the fundamental mechanism is not assumed, and that the constants are easy to determine and interpret. It is suggested that ultimately all of the parameters should eventually be related to the specific breakdown mechanism involved for each material or type of material, but it is emphasized that this relation need not be known to apply the method.

The application of these theories, especially rate process theory and kinetic theory, to any specific group of materials such as paving asphalts requires some further assumptions and mathematical treatments. The following is a brief review of such applications to the analysis of flow behavior of asphalts.

Herrin and Jones (2) applied the absolute rate theory, or rate process theory, to asphalts. Using Eq. 18, they assumed that the values of δ and δ_1 may be considered of the same order of magnitude, and $2\delta/\delta_1$ may be taken ≈ 1. Further, the term $\delta\delta_2\delta_3$ was taken as equal to V_f, the effective volume of the flow unit. Using these assumptions and considering the equation

$$\Delta F = \Delta H - T\Delta S \tag{31}$$

where F is the free energy, H is the heat of activation, T is the temperature in absolute degrees, and S is the system entropy, they found

$$\dot{\gamma} = \dot{\gamma}_o \sinh \frac{\tau}{\tau_o} \tag{32}$$

where $\tau_o = V_f/2KT$ and $\dot{\gamma}_o = (KT/h) \exp(-\Delta H/RT) \exp(\Delta S/R)$. Rewriting the expression for $\dot{\gamma}_o$ in logarithmic form

$$\log \frac{\dot{\gamma}_o}{T} = \log \frac{K}{h} + \frac{\Delta S}{2.303R} - \frac{\Delta H}{2.303R}\left(\frac{1}{T}\right) \tag{33}$$

Then if $\dot{\gamma}_o$ is constant at any given T, the plot of $\log \dot{\gamma}_o/T$ vs $1/T$ should be a straight line. The work of Herrin and Jones showed this relationship to be valid for their material.

It can also be shown that if τ_o is taken as large then the quantity $\dot{\gamma} = \dot{\gamma}_o (\tau/\tau_o)$ may be calculated at any test temperature from the semilog plot, $\dot{\gamma}_o/T$ vs $1/T$ for any selected $\dot{\gamma}_o$. Using this τ_o in the expression $1/\tau_o = V_f/2KT$, the size of the flow unit at any temperature may be found. It can also be shown that ΔS is not a function of temperature, and thus the heat of activation ΔH can be found as the slope of the plot. Since the intercept of the line is ΔS, the free energy of activation ΔF can then be found and is a linear function of temperature.

This analysis applied to one asphalt showed that the flow behavior of asphalt can be predicted using absolute rate theory. It also showed that the flow unit size is much larger than the individual molecules, and that they decrease in size as the temperature increases.

Majidzadeh and Schweyer (3), working with thirteen different asphalts, applied kinetic reaction theory to their data to determine the equilibrium constants, K, as a function of shear rate. For each asphalt, a hyperbolic sine relationship was assumed in the form

$$\dot{\gamma} = A \sinh B\tau, \tag{34}$$

and the constants A and B were determined. The limiting viscosities were found and the equilibrium viscosity for any constant rate of shear was then

$$\eta = \frac{1}{AB \cosh B\tau} \tag{35}$$

which is the inverse of the first derivative of $\dot{\gamma} = A \sinh B\tau$ for any stress level. Eq. 30 may be written in log form as

$$\log \frac{(\eta_o - \eta)^m}{(\eta - \eta_\infty)^n} = p \log \dot{\gamma} + \log K (\eta_o - \eta_\infty)^{m-n} \tag{36}$$

Thus, the slope of the straight line plot of log $(\eta_o - \eta)^m/(\eta - \eta_\infty)^n$ vs log $\dot{\gamma}$ will be p and the intercept at $\dot{\gamma} = 1$ will make possible the calculation of K. Of course, in order to obtain a straight line, the proper choice of m and n must be made. In this case, as with the case of many polymer melts (11), m = 2 and n = 1.

Thus, if the equilibrium constant of a material and its limiting viscosities are known, the viscosity for any shear rate within the range of the study may be calculated knowing one additional point. The only requirements on the material are that it must be represented by a hyperbolic sine relationship, and that the proper choice of the integers m and n can be made such that the log-log plot of $(\eta_o - \eta)^m/(\eta - \eta_\infty)^n$ vs $\dot{\gamma}$ is a straight line.

Physical-Chemical Representation

Early attempts to arrive at a rational explanation for the flow behavior of bitumens assumed a colloidal system. This theory, postulated by Nellensteyn (13), was based on observations of solutions of bitumens in benzene. Mack (6) questions the validity of extrapolation of Nellensteyn findings to a solvent-free material because evidence indicates that asphaltenes are not completely dissolved in benzene but exist in the solution as partially saturated associated particles. This is not compatible with the assumption that the asphaltic bitumens are solutions of asphaltenes in petrolenes which, at low temperatures (less than 120 C), form molecular complexes. Mack shows qualitatively that non-Newtonian flow increases as the aromaticity of the oil constituents decreases. Thus, it would seem that non-Newtonian flow is some function of the concentration of the asphaltenes and aromaticity or the ability of the petrolenes to dissolve the asphaltenes.

This work is substantiated by several studies on asphalt using the electron microscope. Katz and Betu (14) found that photographs of films of bitumens formed from benzene solutions showed associated particles of asphaltenes. Swanson (15) found that to form a homogeneous bitumen film by the same process, the ratio of resins to asphaltenes had to be at least three to one. Finally, if the film is not formed by evaporation of benzene from a bitumen-benzene solution, examination indicates no particles of typical colloidal dimensions.

Although most of the molecular forces in bitumens are dispersion forces of attraction produced by carbon and hydrogen, electron microscope studies seem to indicate that strong polar bonds are also operative. The structural buildup is then somewhat like crystallization in that molecular orientation takes place. On the other hand, unlike crystallization, the operative forces are unable to attract like neighbors because of the relatively large distances over which attractive forces would have to act. Thus, bitumen structure is rather random with unlike molecules attracting each other only if their forces and shapes are such that they can adapt to each other. Molecules with aromatic rings, because of their side groups, lend well to cavity formation in which other molecules, if they are of the right shape, may be trapped. Therefore, again the structure of bitumen is dependent on asphaltene concentration and the aromatic properties of the other constituents.

To relate structure to flow properties, it is necessary to consider the shape of the associated complexes. Considering the internal thermodynamics of the system, change will take place spontaneously only if the free energy is diminished. This decrease is associated with a decrease in surface area, and thus it could be expected that the complexes are spherical in shape. On application of a shear stress the particles elongate into ellipsoids and flow through the oily medium. In the case of Newtonian materials, the association bonds within the particles are too strong to be broken by the applied stress. On application of higher stresses, some point is reached where these bonds begin to break, and continue to break until breakup is in equilibrium with the applied stress. The material then shows Newtonian behavior in two ranges, one of no breakdown (low shear stress) and one of breakdown in equilibrium with stresses (high shear stress). Thus, chemical structure can be related to physical behavior.

THERMAL EFFECTS

Asphaltic materials are thermoplastic and, therefore, will show variation in consistency with change in test temperature. Since climatic variations and construction

conditions represent wide variations in temperature, the prediction of flow behavior with temperature is of great importance. The general method used to represent the viscosity-temperature relationship is some form of graphical plot that produces a straight-line relationship for the particular data. Neppe (16) has listed six different plots along with a description of the equations and useful temperature ranges.

To date, the most commonly used graphical representation of viscosity-temperature data is the Walther plot of log-log viscosity vs log absolute temperature (16). Following the general objective of finding a straight line relationship, this method has been by far the most successful. Another plot, log viscosity vs reciprocal absolute test temperature, was used by the authors in a previous study with good results over a temperature range of 10 C to 60 C (17).

The viscosity-temperature relationship may be explained structurally by considering conditions within the material at low temperatures. In this state the asphaltenes are precipitated from solution and exist as relatively large associated complexes. As the temperature increases, thermal activity forces the individual molecules farther and farther apart. Since the attractive forces diminish rapidly with distance, the complexes subjected to shear stresses begin to break down and thus the viscosity is reduced. Another contributing factor is that at low temperatures varying amounts of oily constituents are held within the asphaltene complexes by association bonds. As the thermal energy increases the strength of the bonds decrease, and the oils are freed to give added lubrication to the system.

Perhaps the most significant advance in the study of temperature effects is the development of the time-temperature superposition principle. The principle was originally developed in the field of polymeric sciences and was successfully used by Ferry (18) to obtain shear diagrams over a wide range of shear rates. The technique is such that the shear diagrams of a temperature-susceptible material like asphalt, determined over a wide range of temperatures, are reduced to a common arbitrary temperature. The result is a shear stress-rate of shear diagram of the material over a wide range of shear rate at that particular temperature.

The procedure involves determining a shift factor, a_T, either analytically or graphically such that when the shear diagram curves for different temperatures are multiplied by their respective a_T's, the curves superimpose on each other in one continuous curve at an arbitrary base temperature. The applicability of the principle to asphaltic materials has been well substantiated. Sisko (19) obtained a master curve of viscosity vs shear rate for a wide range of shear rates. Phillippoff et al. (20) developed a master curve for the dynamic properties of asphalt. The authors (17) have shown a reduced shear diagram over seven decades of shear rate.

GENERAL FLOW MEASURING DEVICES

The measurement of viscosity is a field more widely investigated than the theory of viscosity itself, a fact to which present literature will attest. Viscometers themselves present quite a large variety ranging from small simple rising-bubble types to quite large sophisticated rheometers. The basic problem with most instruments is that they are designed to do a specific job, and in most studies, unless the more sophisticated instruments are available, more than one type of instrument is necessary.

Viscometers are divided into three basic types: rotational, capillary, and miscellaneous. Rotational viscometers may be of the coaxial cylinder type or the cone and plate type. The first is characterized by two concentric cylinders with a small gap between them in which the sample is placed. A constant rotation, or a constant torque is applied to one or both of the cylinders, and the viscosity coefficient is calculated from the torque required to maintain a constant shear, or to keep the other cylinder stationary. These instruments are simple of design and easy to use; however, the data relationships are derived for Newtonian fluids.

For non-Newtonian materials, Brodkey (21) has suggested the following procedure. The correction factor n' may be found by plotting τ vs

$$\frac{\eta^2 r_1^2 \Omega h}{r_1^2 - r_2^2} \tag{37}$$

on a log-log scale where η is the apparent viscosity, r_1 and r_2 are the inner and outer cylinder radii, respectively, Ω is the angular velocity at the face of the inner cylinder, and h is the inner cylinder height. Then for any value of τ, n' is the slope of the line, and

$$\dot{\gamma} = \left[\frac{1 - (r_2/r_1)^2}{n'\left[1 - (r_2/r_1)^{2/n'}\right]}\right]\left[\frac{2r_1^2\Omega h}{(r_1^2 - r_2^2)}\right] \tag{38}$$

If n' is unity, then

$$\dot{\gamma} = \frac{2r_1^2\Omega h}{(r_1^2 - r_2^2)} = \frac{\tau}{\eta} \tag{39}$$

which is the Newtonian case. The measured τ and calculated $\dot{\gamma}$ are then used to construct the shear stress-rate of shear diagram.

The second basic group, capillary viscometers, consists of a fluid reservoir, a capillary tube, a pressure control device, a rate of flow measuring device, and a temperature control device. Rheometers are part of this general group and are distinguished by a piston used to drive the fluid through the capillary tube. Their particular advantage is that their high driving pressures allow viscosity measurements at high shear rates. Orifice viscometers are the simplest and most widely used of the capillary group. Their simplicity makes them highly adaptable to industrial uses, but for research, the difficulties of analyzing the flow mechanism of such a short capillary exclude their use.

Glass capillary tubes are of two types, pressure flow type and gravity flow type. The gravity flow types are generally limited to materials of low viscosity, but are convenient in that the driving force is usually the hydrostatic head of the test liquid itself. The kinematic viscosity may thus be measured directly.

Again, for the capillary viscometer, the relationships are derived for Newtonian materials such that

$$\dot{\gamma}_{wall} = \left(-\frac{dv}{dr}\right)_{wall} = \frac{A}{t} \tag{40}$$

where A is taken as constant and t is fill time, and

$$\tau_{wall} = \dot{\gamma}\left[K_2 (H - h)\, t\right] \tag{41}$$

where K_2 is a calibrated instrument constant and (H - h) is a vacuum head term. For non-Newtonian materials, A is not a constant. Brodkey (21) has suggested the following analysis

$$\dot{\gamma}_{wall} = \left[(3n' + 1)/4n'\right]\,(4\bar{v}/r_o) \tag{42}$$

where n' should satisfy the relationship

$$\tau_{wall} = (-r_o\Delta p/2L) = K'(4\bar{v}/r_o)^{n'} \tag{43}$$

Thus, n' can be obtained from the slope of a log-log plot of $(-r_o\Delta p/2L)$ vs $(4\bar{v}/r_o)$. The corrected shear rate at the wall may then be calculated using n' and its corresponding value of $(4\bar{v}/r_o)$. It should be noted that n' is not necessarily a constant and may have to be found for each value of shear stress at the wall. Shear stress may then be easily

calculated point by point from the relationship

$$\tau = \overset{\circ}{\gamma}\,\eta \tag{44}$$

and the shear stress-rate of shear diagram constructed.

Of all the miscellaneous group, the most useful and widely used is the sliding plate microviscometer. The procedure for this instrument is relatively simple as the geometry is that used to define viscosity. The data, therefore, may be used as taken for both Newtonian and non-Newtonian materials. The instrument produces most favorable results when applied to studies on asphaltic cement. It has the advantage of requiring a small sample, and the viscosity is measured in very thin films of the same order of magnitude as those maintained around aggregates in bituminous mixtures.

MATERIALS AND PROCEDURE

The two asphalt cements used in this study are a 60/70 penetration asphalt cement from a Venezuelan crude and an AC-20 grade asphalt cement used in the "Asphalt Institute Bureau of Public Roads Cooperative Study of Viscosity-Graded Asphalts" coded as B-3056. The results of conventional tests on these asphalts are given in Table 1. The 60-70 penetration asphalt (No. 1) is nearly Newtonian in behavior and the second asphalt (No. 2) is non-Newtonian, as indicated from their viscosity results (Table 1).

Three different instruments were used to obtain viscosity data over a range of temperature of 10 C to 160 C and a range of shear rates of 10^{-4} to 10^{4} reciprocal seconds.

A sliding plate microviscometer, made by Hallikainen Instruments, and a Varian Model G-14 graphic recorder were used to obtain data in a shear rate range of 10^{-4} to 10^{-1} reciprocal seconds and a temperature range of 10 C to 45 C. Specimen preparation and testing were done following the procedure described by ASTM (22) with one exception—each specimen was loaded only once. This exception was used because in the upper range of shear rates, and especially with more complex asphalt, a considerable deformation was necessary to establish a measured constant slope. In many cases this deformation was 200 microns, which represents a one-percent change in area of the plates and was thus used as the maximum deformation permitted on any one specimen.

In order to provide data for low shear rates at higher temperatures, a Haake Rotovisco with coaxial cylinders was used. This instrument and its test procedure is well described by Van Wazer et al. (8). Briefly, the Rotovisco consists of a control unit and a measuring head. The control unit houses electrical circuitry for converting torque to potential difference, the drive motor, and a ten-speed reduction transmission. The measuring head is connected to the control unit with a flexible shaft which acts as both an electrical and mechanical connection.

TABLE 1

STANDARD SPECIFICATION TESTS ON ASPHALTS

Test	Asphalt No. 1	Asphalt No. 2
Specific gravity 77/77 F	1.010	1.020
Softening point, ring and ball	123 F	
Ductility 77 F	150 + cm	250 + cm
Penetration		
100 gm, 5 sec, 77 F	63	30
200 gm, 60 sec, 39.4 F	23.5	
Flash point, Cleveland open cup	455 F	545 F

The sample was introduced into a circular gap between two coaxial concentric cylinders at the base of the measuring head. The cylinders were surrounded by an oil jacket heated to within ±0.1 C of test temperature by a Haake Model F oil bath. The outer cylinder was held stationary while the inner cylinder was caused to rotate at a constant rate by the drive motor through the flexible shaft. Located in the measuring head, between the flexible shaft and the rotating cylinder, is an electrical torsion dynamometer consisting of two coaxial shafts mechanically coupled by a creep-resistant torsion spring. The angular displacement of the spring caused by the torque created on the cylinder immersed in the test material is transmitted electronically through the flexible shaft to the control unit. This torque is then a measurement of viscosity.

The Rotovisco may be equipped with several sizes of inner and outer cylinders of which two, denoted MV and SV, were used depending on the expected viscosity of the material at the particular test temperature. Any one of three measuring heads, 50, 500, or 5000, was used depending on the expected level of stress (the numbers indicate the approximate torque measured in gm-cm). The ten basic rotation speeds may be reduced by 10, 100, or 1000 times using a 10-to-1 and/or 100-to-1 gear reducer in the mechanical transmission line. This provides a minimum shear rate of 3×10^{-3} reciprocal seconds. The minimum test temperature used with this instrument and coaxial cylinders was 45 C. Below this, stress levels exceed the instrument limits.

To obtain the viscosity at high shear rates Cannon-Manning vacuum viscometers were used in conjuction with the Cannon vacuum regulator, and a model H-1 high temperature oil bath. Accuracy is maintained to ±0.5 mm Hg for a range 5-50 cm Hg with the regulator, and to ±0.01 C for a range of 68 to 400 F in the bath. The geometry of the viscometers is described in detail elsewhere (8).

At least three tests were run at each test temperature to describe the range of shear rates available. Test temperatures varying from 45 C to 150 C were used.

RESULTS AND DISCUSSION OF RESULTS

The values of viscosity obtained for the two asphalts used in this study are tabulated in Table 2. As mentioned before, these values were obtained using a capillary, a sliding plate, and a rotational viscometer. Due to the instrument limitations, each type of viscometer could be used only for a certain range of temperature, shear stress, and rate of shear. However, as shown in Figure 1, it was possible to obtain values of viscosity for the asphalts at a test temperature of 45 C with all three viscometers. Figure 1, which shows the variation in the viscosity of asphalt No. 1 with rate of shear, indicates that the three viscometers used gave overlapping data, and there exists a continuity in their results. The slight deviation observed at low rates of shear is believed to be due to an error in the viscosity measurement of the sliding plate viscometer. At the test temperature of 45 C the magnitude of load required to cause flow of the asphalt between the two parallel plates was of the order of a few grams, as shown in Table 2. For such small shear stresses, any small error in the balancing system

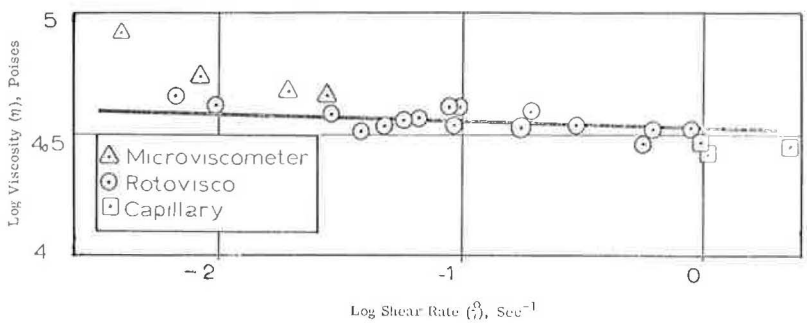

Figure 1. Viscosity vs shear rate for asphalt No. 1 at 45 C with all viscometers.

TABLE 2

VISCOMETRY RESULTS OF ASPHALTS

Description	Shear Stress τ (dynes/cm^2)	Shear Rate $\dot{\gamma}$ (sec^{-1})	Viscosity η Poises
Asphalt No. 1			
T = 5 C	3.30×10^5	6.70×10^{-4}	4.93×10^8
	5.00×10^5	8.55×10^{-4}	5.85×10^8
	7.00×10^5	1.11×10^{-3}	6.31×10^8
	1.00×10^6	1.58×10^{-3}	6.33×10^8
	1.65×10^6	3.08×10^{-3}	5.36×10^8
T = 10 C	1.61×10^5	1.42×10^{-3}	1.13×10^8
	3.50×10^5	2.67×10^{-3}	1.31×10^8
	6.00×10^5	4.68×10^{-3}	1.28×10^8
	1.20×10^5	1.12×10^{-2}	1.07×10^8
	1.65×10^5	1.73×10^{-2}	9.54×10^7
T = 20 C	1.60×10^4	1.31×10^{-3}	1.22×10^7
	3.00×10^4	2.56×10^{-3}	1.17×10^7
	5.50×10^4	4.90×10^{-3}	1.12×10^7
	1.30×10^5	1.23×10^{-2}	1.06×10^7
	3.55×10^5	3.62×10^{-2}	9.81×10^6
T = 25 C	2.50×10^3	8.75×10^{-4}	2.86×10^6
	6.00×10^3	2.29×10^{-3}	2.62×10^6
	1.20×10^4	4.59×10^{-3}	2.62×10^6
	3.50×10^4	1.43×10^{-2}	2.45×10^6
	8.10×10^5	3.43×10^{-2}	2.36×10^6
T = 35 C	8.10×10^2	2.37×10^{-3}	3.42×10^5
	1.50×10^3	4.70×10^{-3}	3.19×10^5
	4.00×10^3	1.39×10^{-2}	2.88×10^5
	9.00×10^3	3.40×10^{-2}	2.65×10^5
	1.63×10^4	6.55×10^{-2}	2.49×10^5
T = 45 C	2.80×10^2	6.48×10^{-3}	4.32×10^4
	9.00×10^2	2.21×10^{-2}	4.07×10^4
	2.80×10^3	7.45×10^{-2}	3.76×10^4
	9.50×10^3	2.67×10^{-1}	3.56×10^4
	3.00×10^4	9.10×10^{-1}	3.30×10^4
T = 80 C	2.38×10^2	7.40×10^{-1}	3.22×10^2
	7.00×10^2	2.17×10^0	3.23×10^2
	1.80×10^3	5.55×10^0	3.24×10^2
	5.50×10^3	1.68×10^1	3.27×10^2
	1.78×10^4	5.43×10^1	3.28×10^2
T = 120 C	4.10×10^2	2.68×10^1	1.53×10^1
	9.00×10^2	5.88×10^1	1.53×10^1
	1.80×10^3	1.19×10^2	1.51×10^1
	4.00×10^3	2.60×10^2	1.53×10^1
	7.70×10^3	5.00×10^2	1.54×10^1
T = 160 C	8.15×10^2	5.22×10^2	1.56×10^0
	1.40×10^3	8.95×10^2	1.56×10^0
	2.80×10^3	1.79×10^3	1.56×10^0
	4.00×10^3	2.56×10^3	1.56×10^0
	5.00×10^3	3.20×10^3	1.56×10^0

TABLE 2 (Cont'd)

VISCOMETRY RESULTS OF ASPHALTS

Description	Shear Stress τ (dynes/cm^2)	Shear Rate $\dot{\gamma}$ (sec^{-1})	Viscosity η Poises
Asphalt No. 2			
T = 10 C	4.00×10^5	2.70×10^{-4}	1.48×10^9
	6.50×10^5	5.15×10^{-4}	1.26×10^9
	9.50×10^5	1.02×10^{-3}	9.31×10^8
	1.30×10^5	1.77×10^{-3}	7.34×10^8
	1.64×10^6	2.68×10^{-3}	6.12×10^8
T = 20 C	1.15×10^5	1.84×10^{-3}	6.25×10^7
	2.20×10^5	4.40×10^{-3}	5.00×10^7
	3.80×10^5	9.35×10^{-3}	4.06×10^7
	7.00×10^5	2.07×10^{-2}	3.38×10^7
	1.16×10^6	4.08×10^{-2}	2.84×10^7
T = 25 C	4.80×10^4	2.08×10^{-3}	2.31×10^7
	8.00×10^4	3.81×10^{-3}	2.10×10^7
	1.50×10^5	8.15×10^{-3}	1.84×10^7
	2.70×10^5	1.62×10^{-2}	1.66×10^7
	4.90×10^5	3.35×10^{-2}	1.46×10^7
T = 35 C	3.28×10^3	2.40×10^{-3}	1.37×10^6
	6.00×10^3	4.77×10^{-3}	1.26×10^6
	1.00×10^4	8.53×10^{-3}	1.17×10^6
	1.80×10^4	1.66×10^{-2}	1.08×10^6
	3.20×10^4	3.15×10^{-2}	1.02×10^6
T = 45 C	7.10×10^2	1.83×10^{-2}	3.88×10^4
	2.00×10^3	4.01×10^{-2}	4.99×10^4
	5.00×10^3	1.39×10^{-1}	3.60×10^4
	1.50×10^4	4.38×10^{-1}	3.42×10^4
	2.90×10^4	8.65×10^{-1}	3.35×10^4
T = 80 C	2.68×10^2	8.80×10^{-1}	3.05×10^2
	7.00×10^2	2.38×10^0	2.94×10^2
	1.80×10^3	5.90×10^0	3.05×10^2
	3.20×10^3	1.03×10^0	3.11×10^2
	7.50×10^3	2.44×10^1	3.07×10^2
T = 120 C	2.28×10^2	1.87×10^1	1.22×10^1
	5.00×10^2	4.10×10^1	1.22×10^1
	1.20×10^3	9.95×10^1	1.21×10^1
	2.50×10^3	2.04×10^2	1.23×10^1
	6.50×10^3	5.35×10^2	1.21×10^1
T = 140 C	2.16×10^3	6.65×10^2	3.25×10^0
	3.40×10^3	1.03×10^3	3.30×10^0
	4.50×10^3	1.36×10^3	3.31×10^0
T = 160 C	1.18×10^3	9.25×10^2	1.28×10^0
	2.00×10^3	1.60×10^3	1.25×10^0
	2.93×10^3	2.32×10^3	1.26×10^0

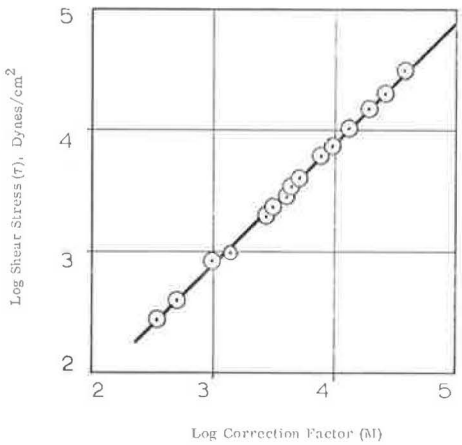

Figure 2. Correction factor vs shear stress for the rotovisco on asphalt No. 1 at 45 C.

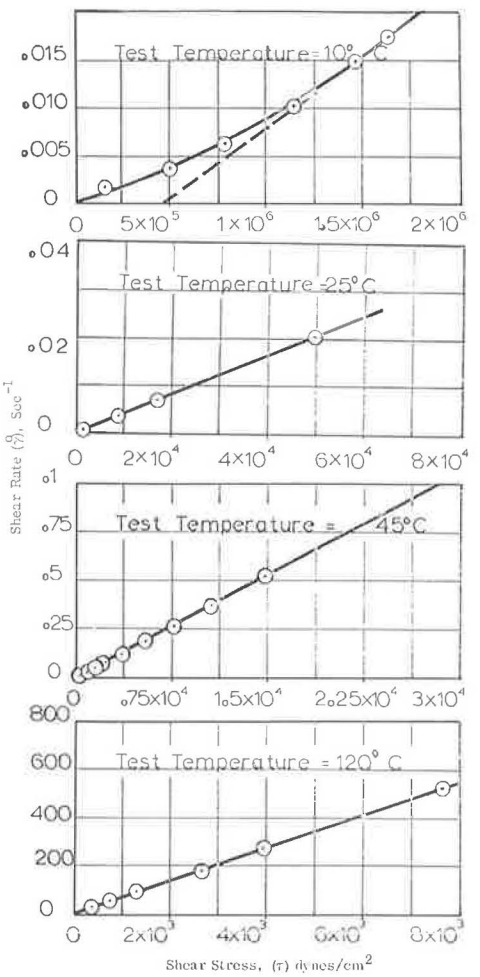

Figure 3. Shear rate vs shear stress on arithmetic scales for asphalt No. 1 at various test temperatures.

of the viscometer would result in significant variation in the calculated values of viscosity.

It was mentioned previously that for capillary and rotational viscometers the calculation of viscosity is based on Newtonian flow. In order to determine the viscosity of non-Newtonian materials, some corrections are necessary. Following the correction procedure as suggested by Brodkey, Figure 2 was constructed. This figure shows the log of shear stress vs log of correction factor M for asphalt No. 1 as obtained by the rotational viscometer where

$$M = \frac{\eta^2 r_1^2 \Omega h}{r_1^2 - r_2^2}. \qquad (45)$$

This figure shows not only that the results generate a straight line, but the slope of such a line is unity, which indicates that the Newtonian analysis is sufficient for determination of viscosity using the rotational viscometer. Similar analysis was used to determine the correction factors for the capillary viscometers, and it was found that for the test temperatures used in this study, the results of capillary viscometers could also be treated as Newtonian.

Figures 3 and 4 show the flow diagrams at different temperatures for the two asphalts used in this study. These figures, which are the plots of rate of shear vs shear stress on arithmetic scales, show that asphalt No. 1 behaves as a Newtonian material at temperatures above 25 C, while asphalt No. 2 exhibits some non-Newtonian behavior up to 45 C. These results when plotted on logarithmic scales generally give straight lines as shown in Figures 5 and 6. This suggests that, over the range of shear stress and for the temperatures used in this study, the shear stress-rate of shear relationship can be approximated by a power formula as

$$\tau = A\,(\dot{\gamma})^n \qquad (46)$$

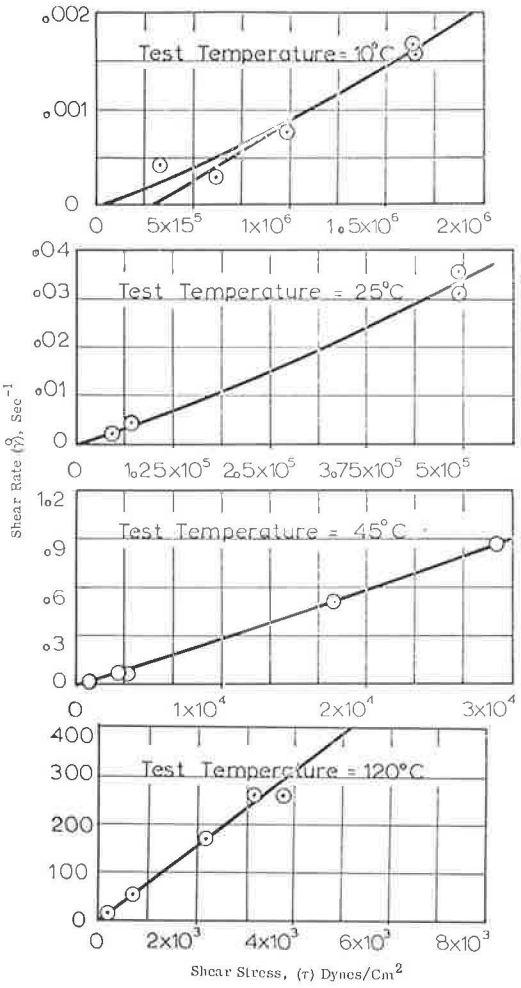

Figure 4. Shear rate vs shear stress on arithmetic scales for asphalt No. 2 at various test temperatures.

where A and n are constants whose values vary with temperature. For both asphalts, at low temperatures the slope of the line is not equal to unity, which indicates that the asphalts exhibit non-Newtonian behavior in that temperature range.

Figures 7 and 8 show master flow curves obtained by reducing the curves of Figures 5 and 6 with a horizontal shift factor (a_T) determined as

$$a_T = \frac{\eta}{\eta_o} \frac{T_o}{T} \qquad (47)$$

where T_o = 318 K is the arbitrary base temperature, and η and η_o are the viscosities of the asphalts at temperatures T and T_o, respectively. The master curves show that when the log $\dot{\gamma}$ vs log τ curves of Figures 5 and 6 were multiplied by the appropriate a_T's, they superimposed in a continuous straight line. These results substantiate the usefulness of the superposition principle in the prediction of the response of materials over wide ranges of shear rate from the results of relatively few tests.

Figure 9 is a plot of log a_T vs $1/T - 1/T_o$ where T_o = 318 K. The curve of each material is made up of two straight-line portions that intersect at a temperature slightly above the softening point of the materials. This inflection is also found in Figure 10, which is a log viscosity vs reciprocal absolute temperature plot for both asphalts. Traxler and Schweyer (24), noticing similar behavior, attributed this change in slope near the softening point to the colloidal nature of the asphalt. They suggested that the colloidal structure of asphalt changes more rapidly with temperature in the region of the softening point than in other temperature regions, which should result in a difference in temperature susceptibility of the material in that region.

TEMPERATURE EFFECT

For Newtonian materials, it is shown that viscosity is not dependent on shear stress and/or rate of shear, and is a constant at any one temperature. For such a material, the relationship showing the temperature dependency of viscosity is independent of shear rate or shear stress, and as shown before (17) this relationship can be expressed satisfactorily by the Arrhenius equation

$$\eta = A \exp(-\Delta E/RT) \qquad (48)$$

where R is the gas constant, and A and ΔE can be considered as constants over limited temperature ranges.

For non-Newtonian materials, however, the viscosity at fixed temperatures is dependent on shear stress or rate of shear. Therefore, in order to develop an expression

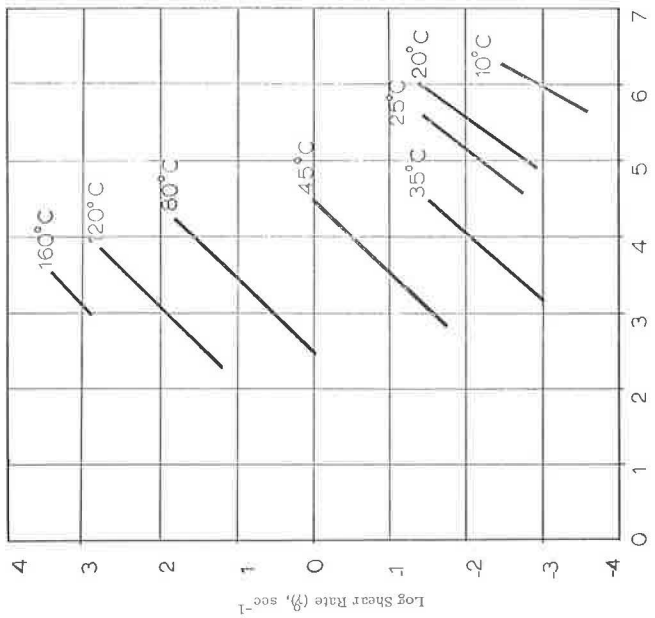

Figure 6. Shear rate vs shear stress on log-log scales for asphalt No. 2 at all test temperatures.

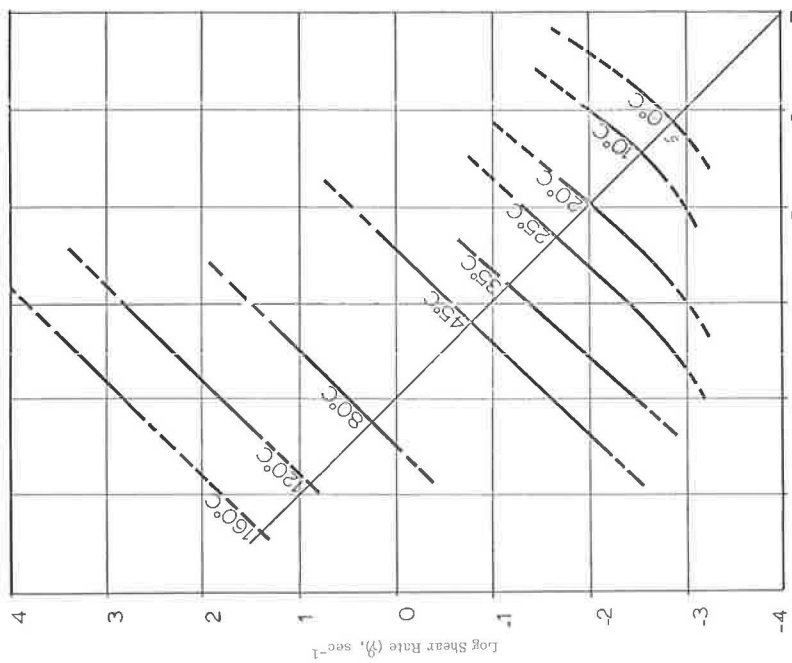

Figure 5. Shear rate vs shear stress on log-log scales for asphalt No. 1 at all test temperatures.

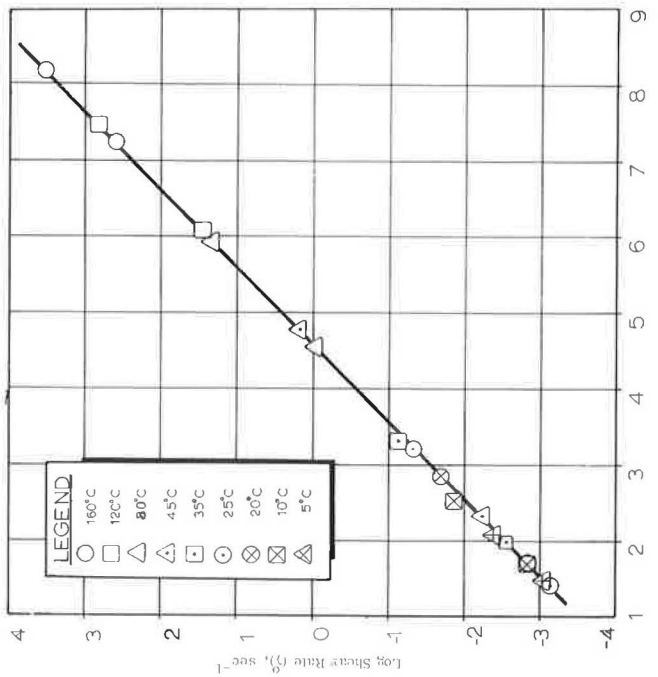

Figure 7. Master flow diagram for asphalt No. 1.

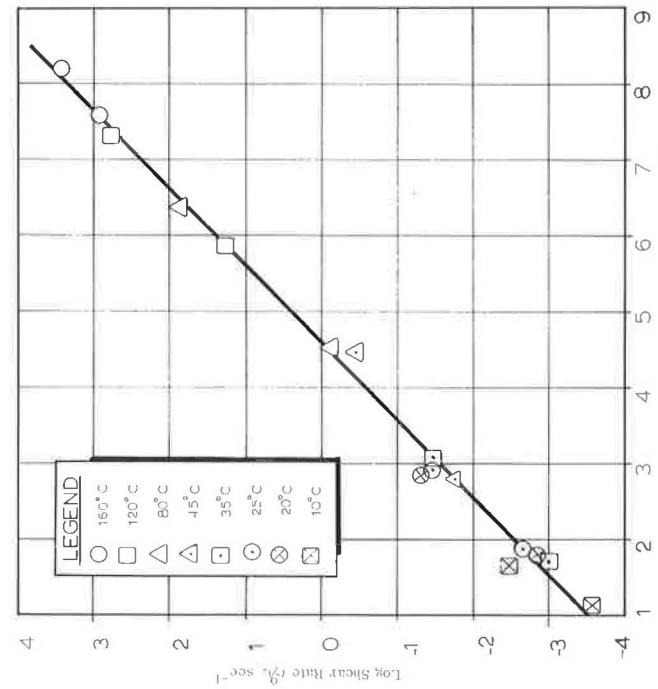

Figure 8. Master flow diagram for asphalt No. 2.

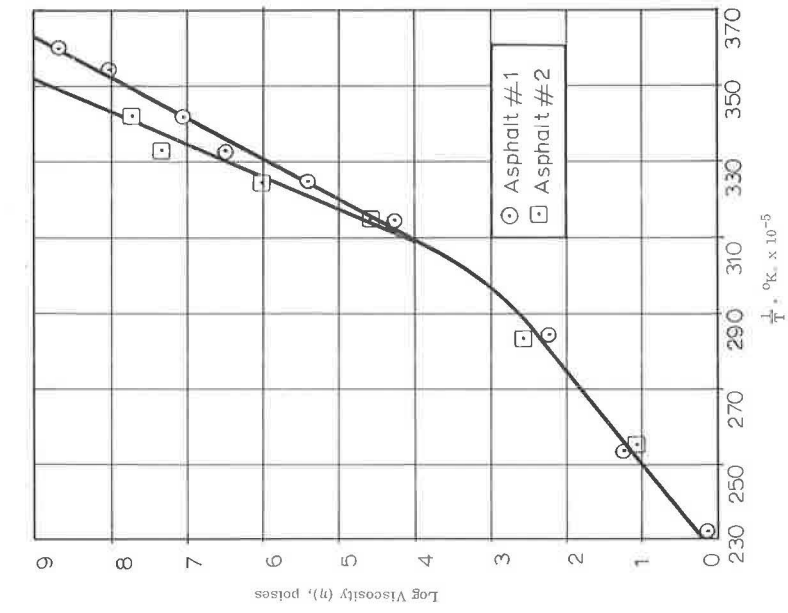

Figure 10. Viscosity vs reciprocal absolute test temperature for both asphalts at a constant power input.

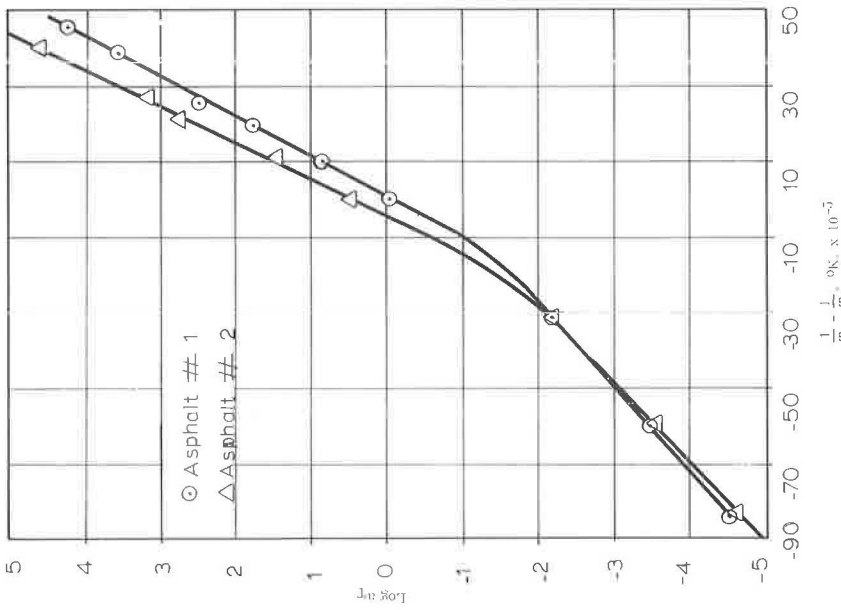

Figure 9. Shift factor vs $1/T - 1/T_o$ for both asphalts at $T_o = 318$ K.

like Eq. 12 to represent the temperature dependency of the viscosity of a non-Newtonian material, either A or ΔE or both must be considered as functions of shear stress or rate of shear. This, in most cases, is avoided by using viscosity at a constant shear rate, a constant shear stress, or a constant power input.

At a fixed shear rate, the viscosity can be expressed as

$$\eta\,(\dot{\gamma},\ T) = \frac{\tau\,(\dot{\gamma},\ T)}{\dot{\gamma}} \tag{49}$$

and at a fixed shear stress as

$$\eta\,(\tau,\ T) = \frac{\tau}{\dot{\gamma}\,(\tau,\ T)}. \tag{50}$$

Formal differentiation of these two equations with respect to temperature at fixed shear stress and fixed shear rate, respectively, results in (23)

$$\frac{(\partial\eta/\partial T)_{\dot{\gamma}}}{(\partial\eta/\partial T)_{\tau}} = \left(\frac{\partial \ln\eta}{\partial \ln\dot{\gamma}}\right)_T + 1 \tag{51}$$

and

$$\frac{(\partial\eta/\partial T)_{\tau}}{(\partial\eta/\partial T)_{\dot{\gamma}}} = 1 - \dot{\gamma}\left(\frac{\partial\eta}{\partial\tau}\right)_T \tag{52}$$

For materials such as asphalt which show a decrease in viscosity with an increase in shear rate and/or increase in shear stress, $(\partial\eta/\partial\tau)_T$ and $(\partial \ln\eta/\partial \ln\dot{\gamma})_T$ are negative.

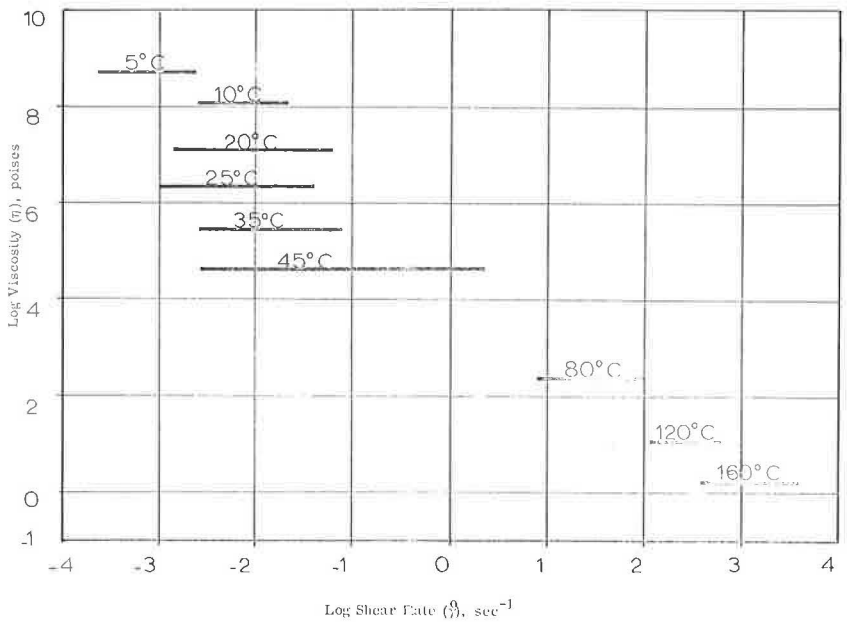

Figure 11. Viscosity vs shear rate for asphalt No. 1 at all test temperatures.

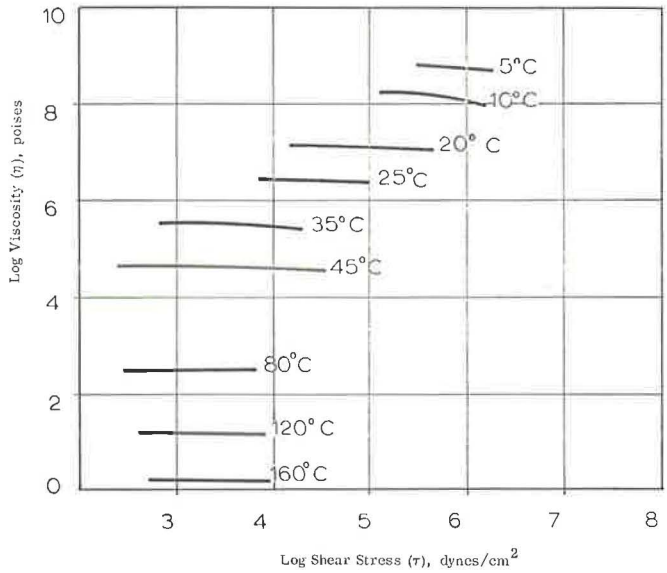

Figure 12. Viscosity vs shear stress for asphalt No. 1 at all test temperatures.

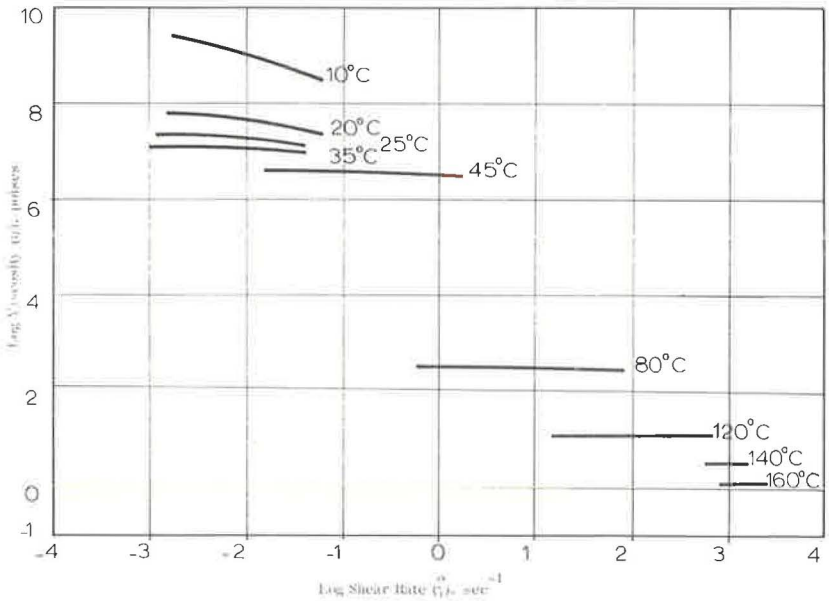

Figure 13. Viscosity vs shear rate for asphalt No. 2 at all test temperatures.

Therefore, the $\left(\frac{\partial \eta}{\partial T}\right)_\tau \Big/ \left(\frac{\partial \eta}{\partial T}\right)_{\dot{\gamma}}$ is larger than or equal to one, or $\left(\frac{\partial \eta}{\partial T}\right)_{\dot{\gamma}} \Big/ \left(\frac{\partial \eta}{\partial T}\right)_\tau$ is smaller than one, which indicates that the temperature variation of viscosity at fixed shear stress is greater than this variation at fixed rate of shear.

The above-mentioned relation can readily be observed from Figures 5, 11, and 12 for asphalt No. 1, and Figures 6, 13, and 14 for asphalt No. 2. Figures 11 and 13 are plots of log viscosity vs log shear rate and Figures 12 and 14 are log viscosity vs log shear

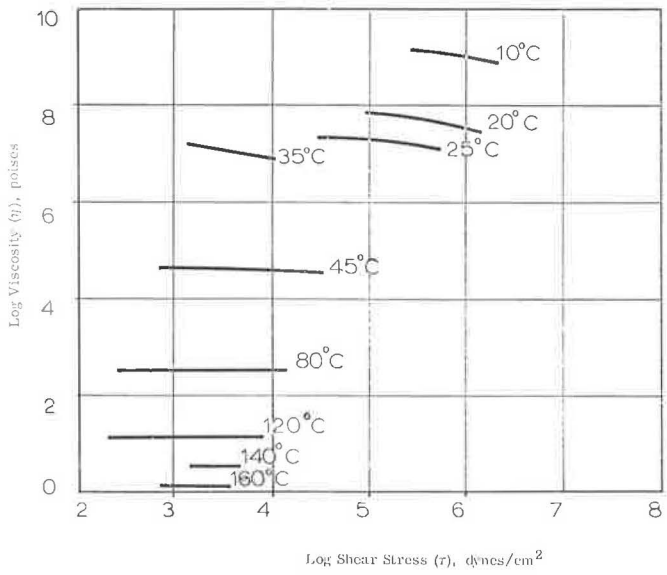

Figure 14. Viscosity vs shear stress for asphalt No. 2 at all test temperatures.

stress for asphalts No. 1 and No. 2, respectively. Using Figures 5 and 6, it can be seen that the variation at fixed shear stress is obtained by a vertical cross plot, whereas the variation at fixed rate of shear is obtained by a horizontal cross plot. It is clear that the distances between the different temperatures are greater along the vertical cross plots than along the horizontal cross plots. This relation results because the slopes of the lines in Figures 5 and 6 are greater than or equal to one, and the plots for different temperatures tend to lie roughly parallel to each other.

EXAMINATION OF HYPERBOLIC SINE FLOW EQUATION

It is believed that the study of the effect of variation of temperature on the viscous behavior of materials may lead to some important information about the molecular structure and mechanism involved in the flow behavior of asphalts. One approach to such a study is the examination of the suggested structural models for the flow of materials through the effect of temperature on their parameters. One of the structural models suggested for the flow behavior of viscous material is the hyperbolic sine equation of Eyring, which has also been applied to flow of asphalt.

Eyring's rate process theory develops a flow relation as given by Eq. 10. This equation can also be written as

$$\vartheta = A \sinh B\tau \tag{53}$$

where, at a fixed temperature, the values of A and B are constant. It is shown by Herrin and Jones (2) that when the flow behavior of asphalt can be represented by this equation, the size of the flow units and their dependency on temperature can be determined using

$$B = \frac{V_f}{2KT} \tag{54}$$

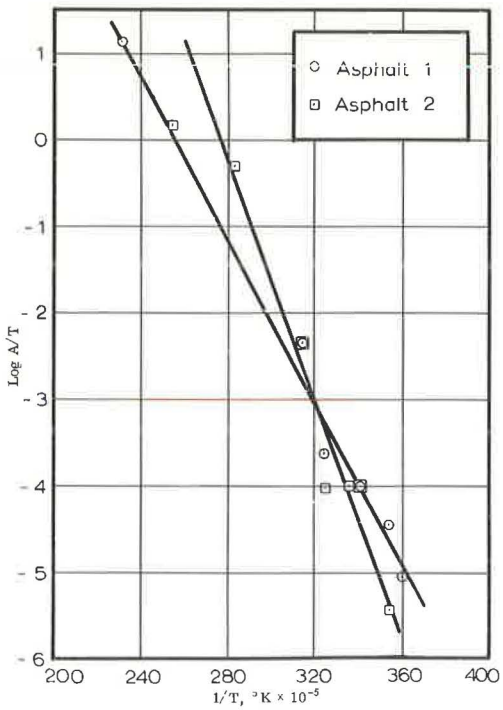

Figure 15. A/T vs reciprocal absolute test temperature for both asphalts.

where V_f is the size of flow unit and T is the absolute test temperature. Furthermore, it is shown that considering a hyperbolic sine relation for flow leads to the calculation of the heat of activation ΔH and the free energy of activation.

In order to examine the validity of such an analysis for the asphalts used in this study, a curve-fitting procedure was used to calculate the values of A and B at each test temperature for the two asphalts. For asphalt No. 1 and No. 2 a plot of log A/T vs 1/T, where T is the absolute temperature, is shown in Figure 15. Herrin and Jones have shown that this plot should be a straight line

$$\log\left(\frac{A}{T}\right) = p - \frac{\Delta H}{2.303R}\left(\frac{1}{T}\right) \qquad (55)$$

where p is a constant over a normal range of temperature, R is the universal gas constant, and ΔH is the heat of activation. This indicates that the slope of the curve representing log A/T vs 1/T is a measure of the heat of activation. Using the corresponding values of B at each temperature for each asphalt, the size of flow units and its variation with temperature were calculated as shown in Figure 16.

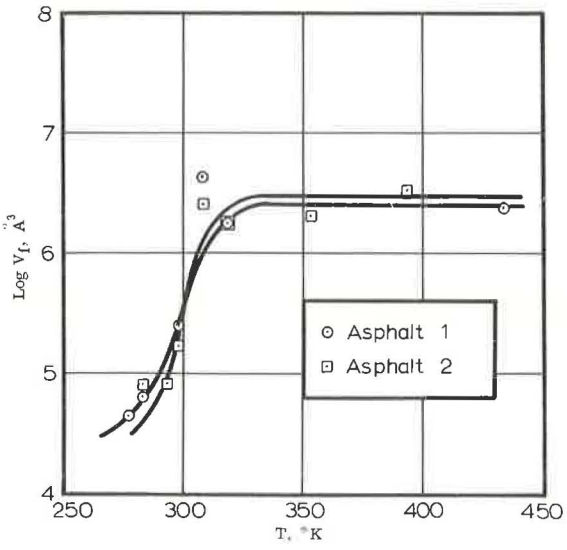

Figure 16. Flow unit volume vs absolute test temperature for both asphalts.

This figure shows that the size of the flow units of both the asphalts increased with temperature to a leveling-off point at about 45 C. According to presently accepted ideas, the flow units should break down and become smaller with increasing temperature. Because of the apparent contradiction shown in Figure 16, a further examination of the validity of using the hyperbolic sine to represent the flow behavior of asphalts was made.

Eyring's flow relation, given by Eq. 18, can be written as

$$\eta = \frac{\tau\delta_1}{2\delta}\left(\frac{h}{kT}\right)\exp\left(\frac{\Delta H - T\Delta S}{kT}\right)\text{cs ch}\left(\frac{\tau\delta\delta_2\delta_3}{2kT}\right) \tag{56}$$

where $\Delta F = \Delta H - T\Delta S$ and $\eta = \tau/\dot{\gamma}$.

Differentiating this expression with respect to 1/T once at constant shear stress and once at constant rate of shear gives

$$\frac{\Delta F_\tau}{R} \equiv \left[\partial \ln\eta/d(1/T)\right]_\tau = \frac{\Delta H}{R} + T - (\tau\delta\delta_2\delta_3/2k)\coth(\tau\delta\delta_2\delta_3/2kT) \tag{57}$$

and

$$\frac{\Delta F_{\dot{\gamma}}}{R} \equiv \left[\partial \ln\eta/d(1/T)\right]_{\dot{\gamma}} = -T + (\Delta H/RT + 1)(2kT^2/\tau\delta\delta_2\delta_3)\tanh(\tau\delta\delta_2\delta_3/2kT) \tag{58}$$

These two equations indicate that if Eyring's flow equation is valid for a material, then the change in logarithm of viscosity, at constant shear stress and/or constant shear rate, with the change in the reciprocal of absolute temperature is not only temperature-dependent but also depends on the shear stress or rate of shear used for the viscosity calculation. Furthermore, these equations show that there exists a certain shear stress at which $\partial \ln\eta/\partial(1/T)$ will go through zero and change sign. For asphaltic materials it is shown that the viscosity always decreases with an increase in shear rate, while the above equations predict a shear stress beyond which the viscosity would start increasing with an increase in shear rate. It is obvious that at shear stresses around this value, the hyperbolic sine function cannot represent the flow behavior of asphalt. In order to obtain an approximate numerical value for this critical shear stress, the following calculated values of the flow unit size and the heat of activation were used at a temperature of 300 K as taken from Figures 15 and 16:

	Temperature °K	H cal/mole °K	V_f $(A^o)^3$
Asphalt No. 1	300	21,400	3.70×10^5
Asphalt No. 2	300	32,000	3.55×10^5

Substitution of these values in the equations and setting the right side equal to zero will result in $\partial \ln\eta/\partial(1/T)_\tau$ and $\partial \ln\eta/\partial(1/T)_{\dot{\gamma}}$ going through zero at $\tau = 7.4 \times 10^5$ dynes/cm^2 for the first asphalt, and $\tau = 2.4 \times 10^6$ dynes/cm^2 for the second asphalt.

Figure 17 shows the variation of $\partial \ln\eta/\partial(1/T)_\tau$ with shear stress for the two asphalts used as determined by Eq. 13. This figure indicates that up to a shear stress of about 10^4 dynes/cm^2 for the asphalts, the behavior of the materials can probably be approximated by a hyperbolic sine relation. This is probably the reason that values of B in $\dot{\gamma} = A \sinh B\tau$ were contradictory. This point is further substantiated by considering that shear stresses below 10^4 dynes/cm^2 could be used only at high temperatures where the behavior of the materials is Newtonian, and the hyperbolic sine relation degenerates into $\tau = \eta\dot{\gamma}$.

The results discussed above indicate that Eyring's hyperbolic sine relation may provide an excellent means to correlate experimental data to a structural analysis of flow

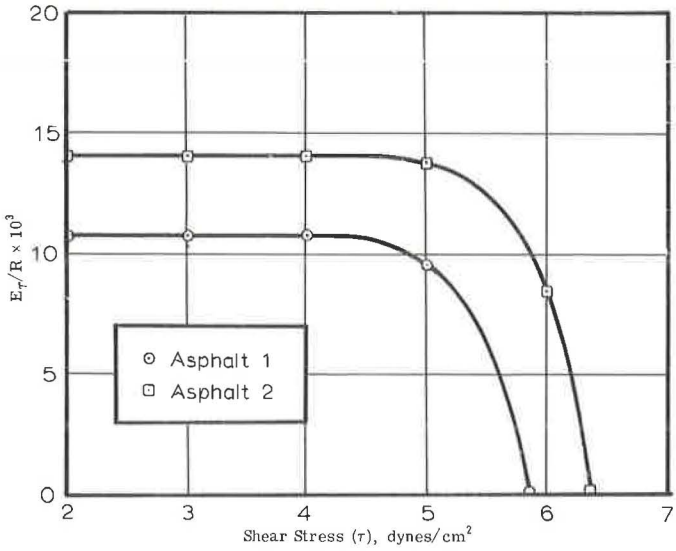

Figure 17. Temperature variation of viscosity at fixed shear stresses according to hyperbolic sine flow equation.

of asphalts in some cases, but not in others. As shown, for both of the asphalts used, such a hypothesis fails to establish conceptually consistant values of the constants necessary to define the expression.

SUMMARY AND CONCLUSIONS

This paper reviews some concepts suggested to analyze the flow characteristics of rheological materials with emphasis on those which are promising in the analysis of flow of asphalts. The suggested concepts are categorized as experimental, mathematical, structural, and physical-chemical. It is shown that for the two asphalts used in this study, it is possible to construct flow diagrams over a wide range of shear stress, rate of shear, and temperature by using three different viscometers and the principle of reduced variables. The application of Eyring's rate process theory to the analysis of asphalt flow is examined and the variation of viscosity, determined at constant shear stress or constant shear rate, with temperature is discussed. From this study, the following conclusions are drawn:

1. The flow data, when obtained by different viscometers, are consistent. Therefore, different viscometers can be used to obtain shear data over a wide range of shear rate or shear stress. The principle of reduced variables will further extend these ranges by reducing the data obtained at different temperatures to an arbitrary base temperature.
2. The temperature dependency of viscosity requires that viscosity variation with temperature at fixed shear stress be larger than that at fixed rate.
3. An examination of the applicability of Eyring's hyperbolic sine relation to analysis of the flow of the two asphalts used reveals that (a) for these two materials there exist critical shear stresses, beyond which the hyperbolic sine relation fails to represent the flow behavior of each material, and (b) when these critical shear stresses are within the experimental range, the flow results cannot be represented by such a relationship.

ACKNOWLEDGMENTS

This research was performed as a part of a project entitled "Durability Characteristics of Asphaltic Materials" sponsored by The Ohio Department of Highways in cooperation with the U. S. Bureau of Public Roads, at the Department of Civil Engineering, The Ohio State University. The authors are grateful to the above agencies for their financial support of this study.

REFERENCES

1. Schweyer, H. E. Asphalt Composition and Properties. HRB Bull. 192, p. 33, 1958.
2. Herrin, M., and Jones, G. E. The Behavior of Bituminous Materials from the Viewpoint of the Absolute Rate Theory. Proc. AAPT, Vol. 32, 1963.
3. Majidzadeh, K., and Schweyer, H. E. Non-Newtonian Behavior of Asphalt Cements. Paper presented at the annual meeting of the AAPT, Feb. 1965.
4. Glasstone, S., Laidler, K., and Eyring, H. The Theory of Rate Processes. McGraw-Hill, New York, 1941.
5. Denny, D. A., and Brodkey, R. S. Kinetic Interpretation of Non-Newtonian Flow. Jour. Appl. Phys., Vol. 33, No. 7, p. 2269, 1962.
6. Hoiberg, Arnold J. (ed.). Bituminous Materials: Asphalts, Tars, and Pitches, Vol. 1. Interscience Pub., New York, 1964.
7. Reiner, Markus. Deformation, Strain, and Flow. Interscience Pub., New York, 1960.
8. Van Wazer, J. R., Lyons, J. W., Kim, K. Y., and Colwell, R. E. Viscosity and Flow Measurement. Interscience Pub., New York, 1963.
9. Bird, R. B., Stewart, Warren E., and Lightfoot, Edwin N. Transport Phenomena. John Wiley and Sons, New York, 1960.
10. Andrade, E. N. da C. Viscosity and Plasticity. Chemical Pub. Co., New York, 1951.
11. Brodkey, Robert S. Unpublished notes.
12. Denny, D. A., Kim, H. T., and Brodkey, R. S. Kinetic Interpretation of Non-Newtonian Flow. Paper presented at the annual meeting of the Society of Rheology, Oct. 1964.
13. Nellensteyn, F. J. Jour. Inst. of Petroleum Technology, 1924.
14. Katz, D. L., and Betu, K. E. Ind. Eng. Chem., 1945.
15. Swanson, J. M. Jour. Phys. Chem., 1942
16. Neppe, S. L. Classification of Bitumens in Asphalt Technology by Certain Rheological Properties. Jour. Inst. of Petroleum, Part 1, p. 38, 1952.
17. Moavenzadeh, F., and Stander, R. R., Jr. Effect of Aging of Asphalt on Its Rheological Properties. Paper presented at the annual meeting of ASTM, June 1965.
18. Ferry, John D. Viscoelastic Properties of Polymers. John Wiley and Sons, New York, 1961.
19. Sisko, A. W. Determination and Treatment of Asphalt Viscosity Data. Highway Research Record 67, p. 27, 1965.
20. Gaskins, F. H., Brodnyan, J. G., Phillippoff, W., and Thelen, E. The Rheology of Asphalt, II. Flow Characteristics of Asphalt. Trans. Society of Rheology, Vol. 4, p. 265, 1960.
21. Brodkey, R. S. Translating Terms for Non-Newtonian Flow. Ind. Eng. Chem., Vol. 54, p. 44, Sept. 1962.
22. ASTM Standards. Proposed Method of Test for Aging Index of Bituminous Materials. 1964.
23. Bestul, A. B., and Belcher, H. V. Temperature Coefficients of Non-Newtonian Viscosity at Fixed Rate of Shear. Jour. Appl. Phys., Vol. 24, No. 6, June 1953.
24. Traxler, R. N., and Schweyer, H. E. Physics, Vol. 7, p. 67, 1936.